Enhanced vector transport of microplastics-bound lead ions in organic matter rich water

Madushika Sewwandi, Hasintha Wijesekara, Anushka Upamali Rajapaksha, Sasimali Soysa, Nadeeshani Nanayakkara & Meththika Vithanage

Check for updates

Enhanced vector transport of microplastics-bound lead ions in organic matter rich water

Madushika Sewwandi[a], Hasintha Wijesekara[b], Anushka Upamali Rajapaksha[a,c], Sasimali Soysa[d], Nadeeshani Nanayakkara[e] and Meththika Vithanage [a,f,g]

[a]Ecosphere Resilience Research Centre, Faculty of Applied Sciences, University of Sri Jayewardenepura, Nugegoda, Sri Lanka; [b]Department of Natural Resources, Faculty of Applied Sciences, Sabaragamuwa University of Sri Lanka, Belihuloya, Sri Lanka; [c]Instrument Center, Faculty of Applied Sciences, University of Sri Jayewardenepura, Nugegoda, Sri Lanka; [d]Department of Physical Sciences and Technology, Faculty of Applied Sciences, Sabaragamuwa University of Sri Lanka, Belihuloya, Sri Lanka; [e]Department of Civil Engineering, Faculty of Engineering, University of Peradeniya, Peradeniya, Sri Lanka; [f]Sustainability Cluster, School of Engineering, University of Petroleum & Energy Studies, Dehradun, India; [g]Institute of Agriculture, University of Western Australia, Perth, Australia

ABSTRACT

Microplastics act as a vector for toxic trace metals and their surface complexation mechanisms under different environmental conditions are poorly understood. The present study evaluates the interaction mechanisms of pristine and aged polyethylene (PE) microplastics with Pb^{2+} in water environments in the presence of $NaNO_3$ and humic acid (HA). The influence of pH, contact time, and concentration of Pb^{2+} on the sorption performances of PE microplastics have also been examined at different ionic strengths (0.001–0.1 M $NaNO_3$), pH (2–9), reaction time (48 h), Pb^{2+} loading concentrations (1–25 mg L^{-1}), and HA concentrations (0.5–2.5 mg L^{-1}). The Pb^{2+} adsorption onto both pristine and aged microplastic showed a gradual increase with increasing pH, reaching maximum adsorption at around pH 5–6. Adsorption of Pb^{2+} onto both PE microplastics decreased at higher ionic strengths and increased at higher HA concentrations suggesting the possible hydrophobic and electrostatic interactions between microplastics and Pb^{2+} ions. Adsorption kinetic data for pristine PE microplastics were well described by fractional power model indicating time-dependent adsorption, whereas aged PE showed rate-limiting chemisorption by fitting with a pseudo-second-order kinetic model. Isotherm equilibrium data for pristine PE microplastics fitted well for the Freundlich model implying favourable physisorption on the heterogeneous surfaces. Both Hill and Freundlich models were the best-fitted models for aged PE microplastics suggesting the involvement of cooperative multilayer physisorption. Desorption of PE microplastics-bound Pb^{2+} was greatly influenced by the solution pH. The ascertaining facts elucidated the vector potential of PE microplastics for Pb^{2+}, impacting their migration and destination in water systems where the adsorption could be influenced by the pH, ionic strength, and dissolved organic matter of the water system.

CONTACT Hasintha Wijesekara ✉ wijesekara@appsc.sab.ac.lk
Supplemental data for this article can be accessed online at https://doi.org/10.1080/03067319.2022.2163896.

1. Introduction

The presence of microplastics in aquatic environments has become a global concern as plastic production, use, especially single-use plastics, and disposal are rising daily [1,2]. Due to the COVID-19 pandemic, plastic usage and haphazard disposal have largely increased and ended up as sources for secondary microplastic formation [3,4]. Chemical (UV radiation and oxidation), physical, and biological processes degrade plastics into microplastics [5]. Primary microplastics are discharged into the environment through the extensive use of personal care products, and accidents such as the X-Press Pearl maritime disaster [6,7].

The high volume-to-surface area ratio and the hydrophobic nature cooperatively support microplastics to act as a vector for various pollutants influencing their migration and destination in water [8,9]. Recent studies have demonstrated the greater affinity of microplastics to both inorganic and organic contaminants [10,11]. Further, it is extensively reported that microplastics have remarkable binding affinities to toxic trace metals such as Cr, Pb, Cd, Cu, Hg, and Ag which ubiquitously exist in the environment due to the direct disposal of domestic, industrial, and municipal waste to the water resources in urban areas [12–14]. Electrostatic interactions, hydrophobic interactions, and surface complexation reactions facilitate the binding of toxic trace metals to microplastic surfaces at different environmental conditions [8,15].

Environmental factors such as pH, dissolved organic matter (DOM), different ion species, temperature, and some features of microplastics (i.e. particle size, number of pores and folds, microplastic type, and degree of ageing) can influence the vector transport ability of microplastics [16,17]. As most toxic trace metals are bound to the surface of microplastics through physisorption, microplastics have a greater chance to release those with a slight change in the environment. Apart from that, microplastics-bound toxic trace metals can be directly ingested by the organisms via food and water [18,19]. Thereafter, the combined effect of toxic trace metals and microplastics may negatively influence both humans and animals [20,21].

With large-scale manufacturing of a wide variety of Pb containing products such as paints, batteries, cosmetics, and ceramics, Pb^{2+} is ubiquitous in aquatic environments [22,23]. Hence, the long-time persistence of Pb^{2+} and microplastics in aquatic systems may promote the interactions between them and thereafter microplastic-bound vector transport. Several studies have focused on the adsorption of Pb^{2+} to different types of microplastics (nylon, polystyrene, polypropylene, and polymethylmethacrylate) and found that they have a higher affinity to bind through electrostatic interactions and surface complexation [24–26].

Lead adsorption onto polyethylene (PE) microplastics has relatively less investigated though PE microplastics are the most found in aquatic environments [27]. Hence, examining the adsorption process of Pb^{2+} onto PE microplastics is timely important. Further, mechanisms of Pb^{2+} adsorption onto aged microplastics are scarce. Especially, in-depth studies focusing on Pb^{2+} adsorption of both pristine and aged microplastics from the same polymer are not available in the literature. Therefore, parallel assessment of both adsorption and desorption possibilities of PE microplastics would be an added advantage to fill the existing knowledge gap. The objectives of the present study were to (a) determine the adsorption capacities of pristine and aged PE microplastics for Pb^{2+}

adsorption in the presence of various environmental factors such as pH, dissolved organic matter, and competitive ions; (b) postulate sorption mechanisms of Pb^{2+} and PE microplastics; and (c) study the desorption dynamics of microplastic-bound Pb^{2+} in relation to pH.

2. Materials and methods

2.1. Materials and chemicals

Pristine PE microplastics (size ~100 μm Microscrub®) were purchased from MicroPowders, Inc. Tarrytown, New York, USA. Aged PE microplastic debris was obtained by exposing a PE film to sunlight for a month. The weathered film was first cleaned with deionised water and then ground. Finally, ground particles were sieved through stainless steel sieve with a 250 μm mesh screen to collect <250 μm microplastics. The solution pH was adjusted by using 0.1 M nitric acid and 0.1 M sodium hydroxide. All chemicals are analytical grade. Sodium nitrate ($NaNO_3$) and humic acid (HA) were obtained from Sigma-Aldrich, USA. Lead nitrate ($PbNO_3$) was purchased from Riedel-de Haën, Seelze, Germany. A stock solution of Pb^{2+} (1000 mg L^{-1}) was made by initially dissolving the solid in deionised water. The sodium salt of HA was used to prepare a 1000 mg L^{-1} of stock solution in ultrapure water. Additionally, a 5 M $NaNO_3$ stock solution was prepared to maintain different ionic strengths.

2.2. Microplastics characterisation

Solution pH at point of zero charges (pH_{zpc}) of the PE microplastic surfaces was calculated by a surface titration with 0.05 M HNO_3 and 0.1 M NaOH for 1 g L^{-1} of PE microplastics dosage at different ionic strengths (0.1, 0.01, and 0.001 M $NaNO_3$). The surface morphology of PE microplastics was determined by Field Emission Scanning Electron Microscopy (FE-SEM) at 15 kV (Hitachi SU6600, Japan). The surface functional group identification of PE microplastics and Pb^{2+} adsorbed microplastics (dried samples) was conducted by Fourier Transform Infrared-Attenuated Total Reflectance (FTIR-ATR) spectroscopy analysis (BRUKER, ALPHA II, Germany) in the range 500–4000 cm^{-1} with 32 scans and resolutions of 4 cm^{-1}.

2.3. Batch sorption experiments

2.3.1. Effect of pH, ionic strength, and DOM on Pb^{2+} adsorption to PE microplastics
A weight of 0.01 g pristine PE microplastics was separately taken into 30 mL glass vials. After spiking with an initial concentration of 5 mg L^{-1} of Pb^{2+} into a glass bottle containing ultrapure water, the pH was adjusted to a range of 2–8 using 0.1 M HNO_3 or 0.1 M NaOH [25]. At each pH, 10 mL of the suspension was dispensed into glass vials to maintain a 1 g L^{-1} microplastics dosage and kept in a shaking water bath (GEMMYCO VCW-012S, Taiwan) for 48 h at a speed of 150 rpm at 25°C. The final pH was recorded, and the samples were filtered through 0.22 μm PTFE filters. The amount of remaining Pb^{2+} was determined by analysing the filtrate by the Agilent 4210 Microwave Plasma Atomic Emission Spectroscopy (MP-AES) at the wavelength of 363.9 nm. The control experiment was conducted without microplastics. The effect of ionic strength and the effect of DOM on

Pb^{2+} adsorption were examined by repeating the pH edge experiment at the same pH range. The ionic strength experiments were performed with 0.001, 0.01, and 0.1 M concentrations of $NaNO_3$. Different HA concentrations (0.5, 1.5, and 2.5 mg L^{-1}) were used to study the effect of DOM. The same pH edge experiments (i.e:)were repeated for the aged PE microplastics.

2.3.2. Kinetic experiments

Adsorption kinetic experiments were conducted with an initial Pb^{2+} concentration of 5 mg L^{-1} at the optimum pH range derived from the pH edge experiment (pH 5–6) and the optimum ionic strength (0.001 M). A dosage of 1 g L^{-1} of pristine PE microplastics was maintained, and samples were shaken at the speed of 150 rpm at 25°C. Samples (10 mL) were withdrawn at the time intervals of 10–2880 min and filtered through 0.22 μm PTFE filters. The same kinetic experiment was repeated for aged PE microplastics.

2.3.3. Isotherm experiments

Adsorption isotherm experiments were carried out with Pb^{2+} concentrations ranging from 1 to 25 mg L^{-1} at 0.001 M $NaNO_3$ ionic strength in glass vials. A 1 g L^{-1} of pristine PE microplastics dosage was used and the solution pH was maintained at pH 5–6. All the vials were placed in a horizontal shaker for 48 h of equilibrium time as per the observations determined by the kinetic experiment. The isotherm experiment was repeated with HA 2.5 mg L^{-1} to analyse the influence of DOM. The same procedure was performed for the aged PE microplastics. The kinetic and isotherm data were modelled, and the parameters were determined using Origin statistical computer software (version 8.0).

2.4. Desorption experiment

Desorption studies were conducted using both pristine and aged PE microplastics that were used in the kinetic experiments (i.e. PE microplastics retained in 5 mg L^{-1} of Pb^{2+} for 48 h at pH 5–6). The PE microplastics were filtered through glass microfiber filters and dried overnight. The remaining Pb^{2+} concentrations of the samples were determined by analysing the filtrates. The dried Pb^{2+} adsorbed PE microplastics (0.05 g) were added to 50 mL of deionised water at three different pH conditions; 3, 5, and 7 [25]. Then, the samples were horizontally shaken at the speed of 150 rpm at 25°C for 2 h. The same desorption experiment was repeated to assess desorption after 24 h. To maintain the quality and accuracy of the experimental data, each experiment was conducted with control samples for three times.

3. Results and discussion

3.1. Surface characterisation of PE microplastics

3.1.1. Surface morphology, surface area and degree of crystallinity

Surface morphology, surface area, and degree of crystallinity of microplastics are the most significant inherent factors that can correlate with adsorption capacity [28,29]. The charge of the microplastic surface can influence metal ion adsorption. The pH_{pzc} for pristine and aged PE microplastics was determined as pH 4.42 and pH 3.82, respectively (Figure S1).

Therefore, throughout the experimental conditions above pH 4.42, the surface of both pristine and aged microplastics can be expected to show a net negative charge and vice versa [25]. According to Figure 1(a), pristine PE microplastics were in different shapes and sizes while the surface likely consisted of more pore spaces and cavities due to the different irregular folds on the surface. Besides, as shown in Figures 1(b), differently sized and shaped pores could be observed on the aged microplastic surface. Thus, both pristine and aged microplastics seem to be rough and coarse (Figure 1(a,b)). Although both surfaces of pristine and aged consist of pores, aged PE microplastics appeared to be coarser than pristine because of the well-distributed pores on their surfaces. However, all pores and voids on the surface of PE microplastics collectively facilitate the adsorption providing broaden surface area to the adsorbates [9]. Low degree of crystallinity of PE microplastics acts vital a role in metal adsorption facilitating the mobilisation of metal ions into the loosely arranged polymer chain [30,31]. Further, the presence of a higher amorphous region rather than the other types of microplastics (PVC and PS) provides an extended binding ability to the PE polymer structure through Van der Waals interactions.

3.1.2. FTIR-ATR analysis of PE microplastics

FTIR spectra of pristine and aged PE microplastics are shown in Figure 1(c) and they were well recognised with the characteristic bands at 2916 cm^{-1} for $-CH_2$ asymmetric stretching, 2846 cm^{-1} for $-CH_2$ symmetric stretching, 1465 and 1419 cm^{-1} for $-CH_2$ bending deformation and 717 cm^{-1} for C-H rocking deformation [32]. Aged PE microplastics exhibited two new absorption bands at 1712 and 1087 cm^{-1} assigned to C=O and C-O-C stretching vibrations, respectively [33,34]. The stretching vibrations of C=O and C-O-C indicate the surface oxidation of the aged PE polymer chain during the natural ageing process and the formation of aldehydes and ketone intermediates [25,35]. Moreover, a new absorption band appeared at 1080 cm^{-1} and an intensified band at 1087 cm^{-1} in Pb^{2+} loaded pristine and aged PE microplastics respectively attribute to C-O stretching vibrations (Figure S2). They likely indicate that some interactions between the C-O and Pb^{2+} have occurred via surface complexation [25]. Thus, the weak absorption band of C-H bending at 846 cm^{-1} in the spectrum of pristine PE microplastics was shifted to 871 cm^{-1} after loading Pb^{2+} ions (Figure S2a). This indicates the decrease of C-H bond length during the adsorption process likely showing the surface complexation of Pb^{2+} ions on the PE chain at the C-H position [36]. In the present study, Pb^{2+} adsorption onto PE microplastics was confirmed by the shifted and intensity-increased absorption bands. Accordingly, the overall adsorption of Pb^{2+} ions on PE microplastics is likely determined by surface complexation.

3.2. Effect of solution pH

The behaviour of Pb^{2+} adsorption on both pristine and aged PE microplastics was remarkably varied with the increase of pH from 2 to 8 showing a maximum adsorption capacity around the pH range of 5 to 6 (Figures 2 and 3). Precipitation of $Pb(OH)_2$ ($k_{sp} = 1.43 \times 10^{-20}$) occurred at higher pH values (above pH 6). The prominent dependency of Pb^{2+} adsorption on pH may be due to either surface potential change or different speciation of Pb at different pH levels. As the determined pH_{pzc} for both pristine and aged PE microplastics were around pH 4.0, PE microplastics exhibited a net negative surface charge above pH 4.0
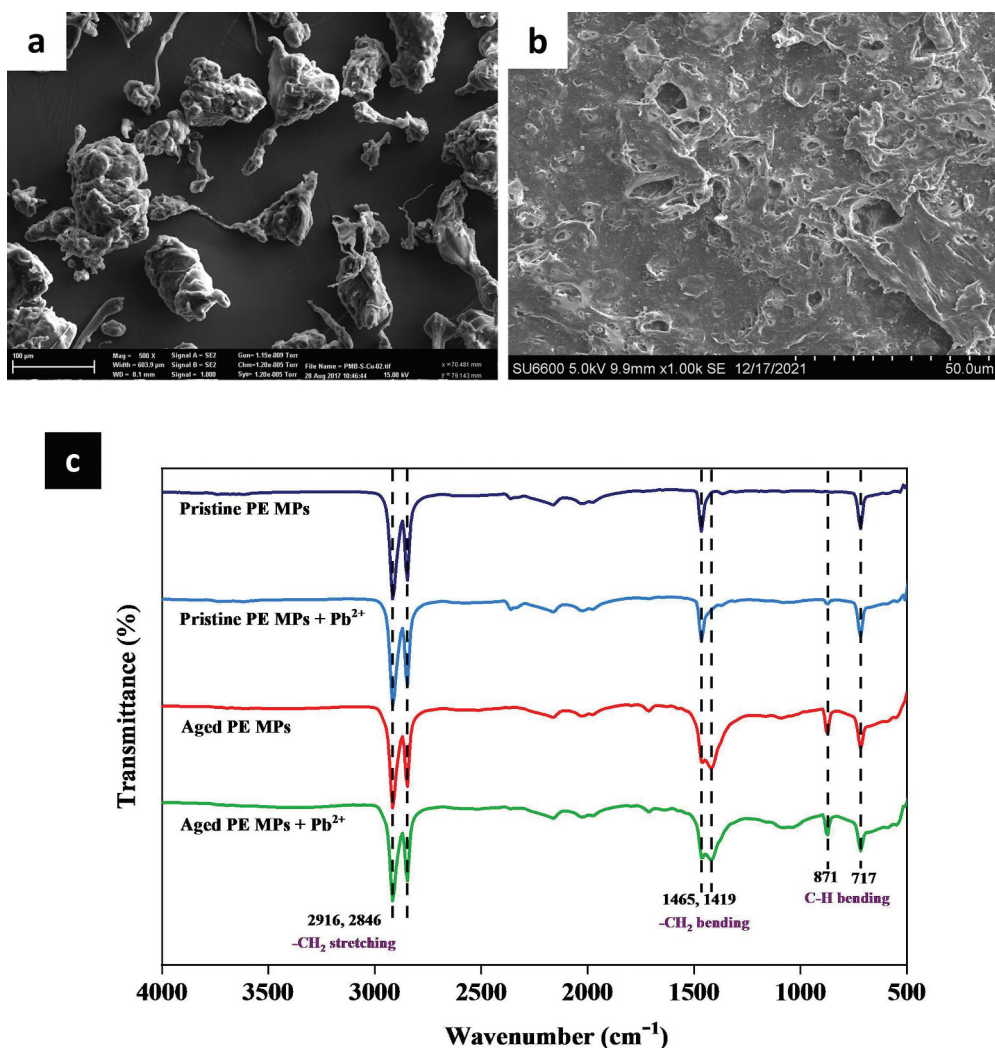
Figure 1. SEM images of the PE microplastics, (a) magnification of 500× for pristine PE microplastics, (b) magnification of 1000× for aged PE microplastics, and (c) FTIR-ATR spectra of the pristine PE microplastics, aged PE microplastics, and Pb^{2+} adsorbed pristine and aged PE microplastics from 500 to 4000 cm^{-1} wavenumber.

for Pb^{2+} adsorption during the experiment. Throughout the experimental conditions (pH 2–8), Pb predominantly appears in the solution as Pb^{2+} and slightly as $Pb(OH)^+$ [37]. Therefore, the noticeable increase in Pb^{2+} adsorption might facilitate by electrostatic interactions between positively charged Pb ions and negatively charged surface of PE microplastics.

Several studies have stated that higher Pb^{2+} adsorption at high solution pH might be ascribed to the electrostatic attractions and the surface complexation [37–39]. In the present study, when Pb^{2+} and PE surface has electrostatic repulsive forces to each other, no considerable adsorption appeared in the absence of $NaNO_3$ and HA, thereby indicating electrostatic interaction may be the main factor determining the overall sorption. Even so, a slight increase of the adsorption at pH conditions, <pH 4.42 in the presence of $NaNO_3$
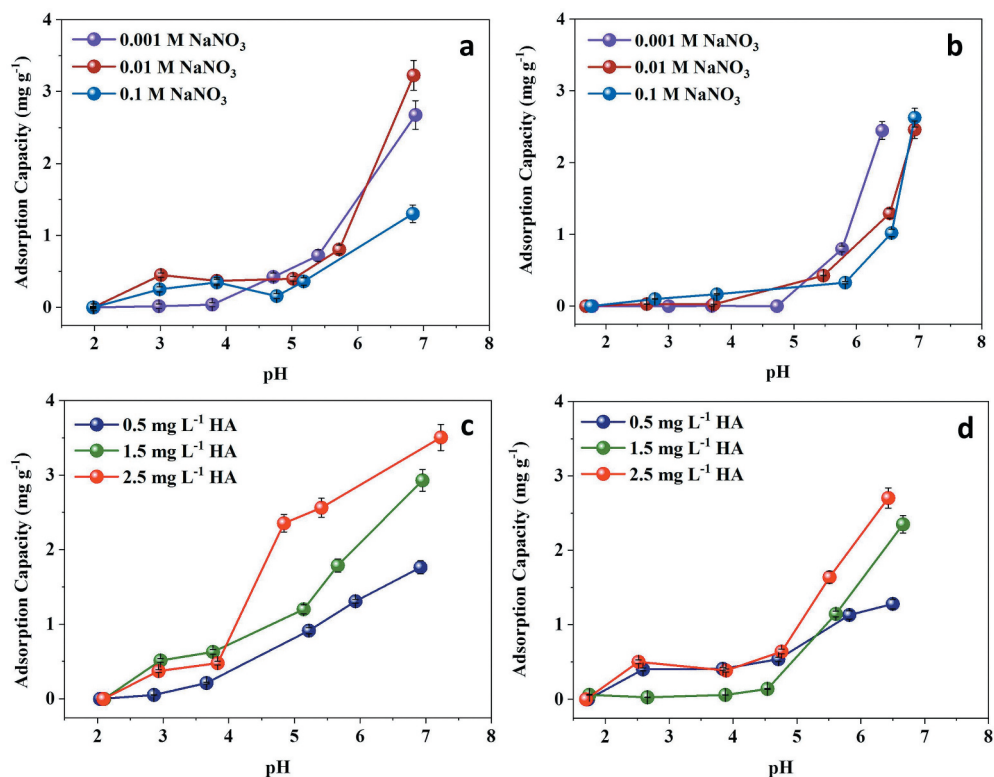
Figure 2. Pb^{2+} adsorption variation of (a) pristine PE (b) aged PE in the presence of 0.001, 0.01, and 0.1 M NaNO$_3$, (c) pristine PE (d) aged PE in the presence of 0.5, 1.5, and 2.5 mg L^{-1} of humic acid (HA) in pH 2–8.

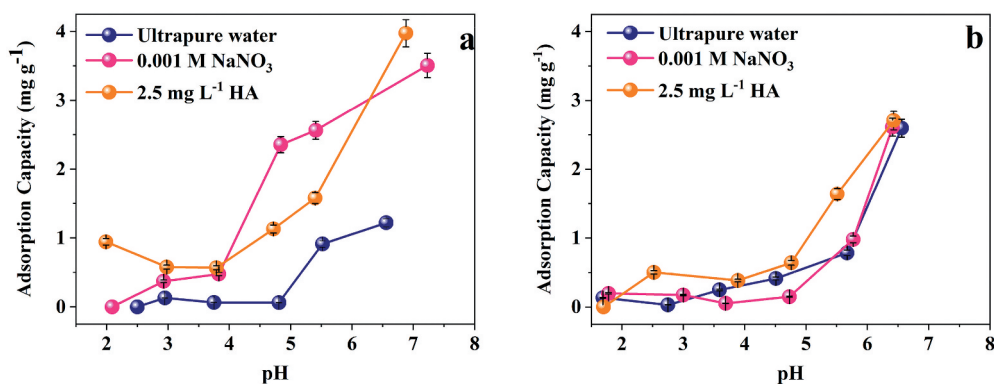**Figure 3.** Pb^{2+} adsorption variation onto (a) Pristine PE (b) aged PE in the presence of ultrapure water, 0.001 M NaNO$_3$, and 2.5 mg L^{-1} humic acid (HA) in pH 2-8.

and HA might attribute to surface complexation between Pb^{2+} and PE microplastics. Accordingly, pH performs a vital role in the Pb^{2+} uptake process onto PE microplastics influencing surface charge and speciation of Pb.

3.3. Effect of ionic strength

The dissolved salt ions in the natural water have a higher tendency to influence the metal ion adsorption to the microplastics. Adsorption of Pb^{2+} exhibited a decreased trend with an increase in $NaNO_3$ concentration from 0.001 M to 0.1 M, reaching maximum adsorption at 0.001 M $NaNO_3$ concentration at pH 5–6 (Figure 2). When $NaNO_3$ concentration was increased from 0.001, 0.01, and 0.1 M, adsorption capacities for pristine PE microplastics were reduced from 0.90 mg g^{-1} to 0.86, 0.68, and 0.54 mg g^{-1}, respectively. Adsorption capacities for aged PE microplastics were dropped down from 0.73 mg g^{-1} to 0.30, 0.44, and 0.59 mg g^{-1}. Similarly, in previous studies, the adsorption performance of PE pellets for toxic trace metals (Co, Pb, Cu, Cd, Cr, and Ni) significantly decreased in seawater than in river water [40,41].

3.4. Effect of the DOM concentration

The overall Pb^{2+} adsorption to both pristine and aged microplastics was remarkably enhanced with the treatment of HA reaching maximum adsorption in the presence of 2.5 mg L^{-1} of HA concentration at pH 5.5. When HA concentration was increased from 0.5, 1.5, and 2.5 mg L^{-1}, Pb^{2+} adsorption capacities were increased from 0.90 mg g^{-1} to 1.06, 1.61, and 2.61 mg g^{-1}, respectively (Figure 2(c,d)). In addition, the maximum Pb^{2+} adsorption capacities for aged PE microplastics were enhanced from 0.73 mg g^{-1} to 0.95, 1.04, and 1.62 mg g^{-1}, respectively in the presence of 0.5, 1.5, and 2.5 mg L^{-1} of HA concentrations. Similarly, few studies have observed an enhanced Pb^{2+} and Cd^{2+} adsorption to microplastics with the increase in HA concentrations [15,42]. The gradual increase in adsorption capacities even at low HA concentrations than in the absence of HA likely indicates that HA might promote the adsorption interacting with either PE microplastics or Pb^{2+} ions.

3.5. Effect of the components in the sorption medium and possible sorption mechanism

The comparison of Pb^{2+} adsorption on PE microplastics at optimum ionic strength (0.001 M) and HA concentration (2.5 mg L^{-1}) likely indicates that changing the components present in the sorption medium greatly affected the Pb^{2+} adsorption than plain ultrapure medium (Figure 3). Polyethylene microplastics exhibited enhanced Pb^{2+} adsorption performance in the presence of either different ionic species (NO_3^- and Na^+) or dissolved organic matter (HA) than alone with ultrapure water. Pristine PE microplastics showed remarkable adsorption in the presence of different ionic species when compared to HA (Figure 3(a)). Aged PE microplastics showed a different behaviour from pristine PE microplastics as they preferentially absorbed Pb^{2+} onto their surfaces when the sorption medium was rich with organic matter (Figure 3(b)). Consequently, either pristine or aged PE microplastics in water systems polluted from various organic matters and ionic species can boost the ability to support the vector transport of Pb^{2+}.

Increasing the ionic strength may have reduced the activated binding sites of PE microplastics as cations (Na^+) in the sorption medium start to electrostatically interact with the negatively charged surface by occupying them. Therefore, the dropped-down charge

equilibrium of the PE surface directly influences the Pb^{2+} adsorption. The reduced Pb^{2+} adsorption with the induction of competing ions likely indicates that electrostatic interactions are the predominant way of binding Pb^{2+} to the negatively charged PE surface [43]. Further, the negativity of the PE surface is further confirmed by the reduction of sorption capacities of Pb^{2+} at higher ionic strengths. It has already been proven that Pb^{2+} adsorption can compensate as PE microplastics start to agglomerate in the water system face to face or side to side blocking the available adsorption sites [44]. With the increase of ionic strengths, Na^+ and NO_3^- ions commence penetrating the electrical double layer aggregating close to the PE microplastic surface, thereby reducing electrostatic potential and dropping down the metal adsorption [25]. Further, Na^+ and NO_3^- ions may interrupt Pb^{2+} adsorption by acting as an electrostatic screen between the PE surface and the Pb^{2+} ions [45,46]. However, Holmes, Turner and Thompson observed a slightly increased chromium adsorption for PE microplastics, in the presence of higher ionic strengths [41]. Therefore, when considering the overall effect in current and previous studies, the influence of ionic strength on the metal ions adsorption behaviour may depend on the type of microplastics, toxic trace metal, and competitive ionic species in the sorption medium.

The sorption mechanism of Pb^{2+} onto PE microplastics in the presence of HA can be postulated based on the surface charge of the microplastics and the speciation of Pb^{2+} and HA at the optimum pH range (pH 5–6). Phenolic and carboxylic groups present in HA begin to dissociate when increasing the solution pH [47]. Accordingly, as illustrated in Figure 4, the anionic ends of those groups would attract positively charged Pb^{2+} via electrostatic interactions at pH 5–6 [48,49]. Hydrophobic regions of HA have a greater affinity to interact with microplastics through hydrophobic interactions increasing their surface hydrophobicity. If HA predominately interacts with the microplastic surface through hydrophobic interactions, Pb^{2+} adsorption onto microplastic surfaces through electrostatic interactions would start to drop down due to the complexation between HA and microplastics and thereby form a hindrance between metal ions and surface [25,50]. Accordingly, the enhanced adsorption at higher HA concentrations in the current study might be governed by the combined effects of both HA-PE microplastics and HA-Pb^{2+} complexes offering a more hydrophobic surface for adsorption and redistributing Pb^{2+} ions in the solution, respectively. However, the extent of Pb^{2+} adsorption depends on the concentration of HA in the sorption medium.

3.6. Adsorption kinetics

The adsorption kinetic behaviour of the two types of PE microplastics was entirely different from each other (Figure 5(a)). Without reaching an equilibrium sorption capacity within 32 h, Pb^{2+} adsorption for pristine PE microplastics gradually increased with time. Lead ion adsorption onto aged PE microplastics approached nearly 1.2 mg g^{-1} equilibrium adsorption capacity within 2 h showing an increasing trend at the beginning of the adsorption. By applying different kinetics models for the adsorption process, the partitioning governing factors such as type of diffusion (internal, external, or pore diffusion), surface sorption, and mass transfer chemical reaction can be elucidated [51]. Accordingly, Pb^{2+} adsorption behaviour for pristine PE microplastics was best fitted with the fractional power kinetic model with R^2 of 0.983 ascribing a time-dependent adsorption [52,53] (Table 1). However, the fractional power model does not deeply describe the sorption
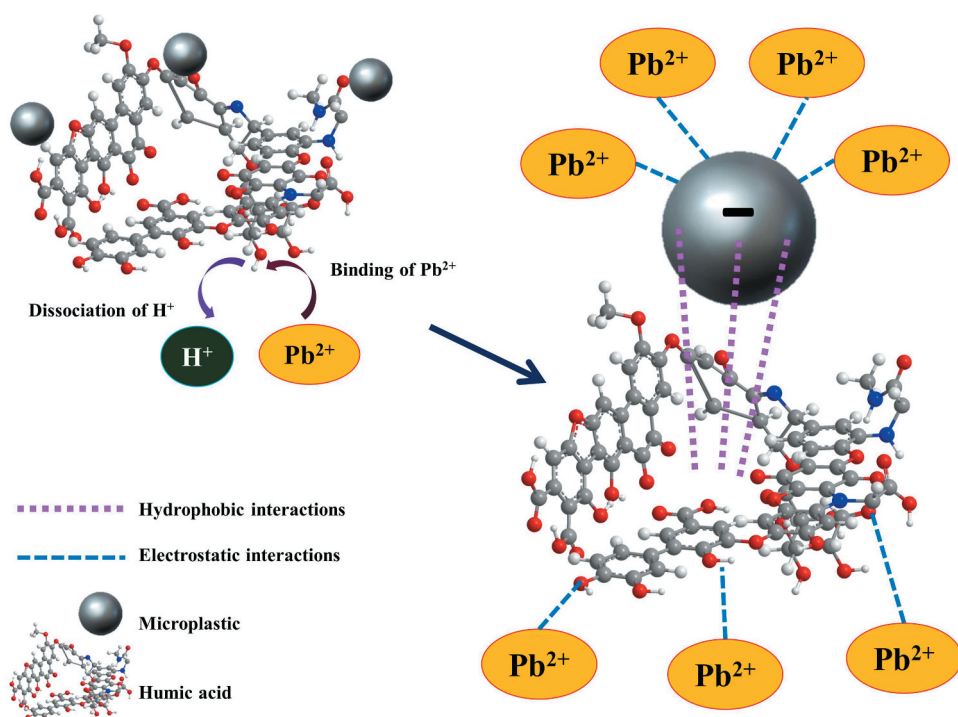
Figure 4. Postulated adsorption interactions between Pb^{2+}, PE microplastics, and humic acid at pH 5–6.
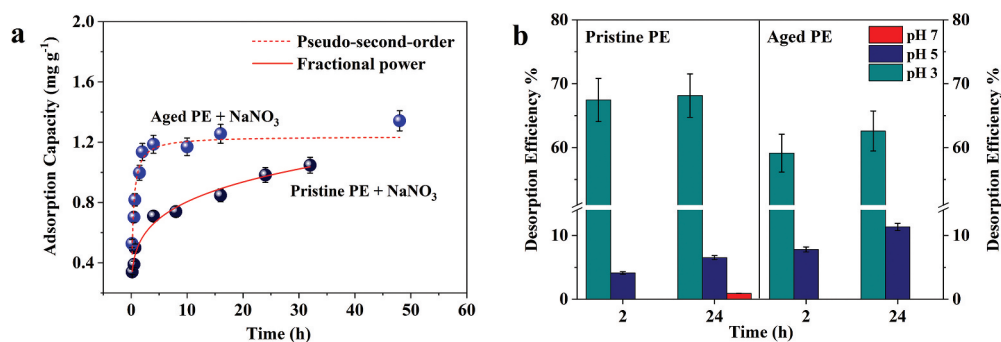

Figure 5. (a) Pseudo-second-order and fractional power kinetic models for Pb^{2+} adsorption on pristine and aged PE microplastics at an initial concentration of 5 mg L^{-1} at pH range 5–6 in the presence of 0.001 M NaNO$_3$ and the solid lines represent the calculated results using.

process for pristine PE microplastics. Therefore, contact time would be the rate-limiting factor for Pb^{2+} adsorption onto pristine PE microplastics.

Moreover, Pb^{2+} adsorption onto aged PE microplastics could be well described by the pseudo-second-order kinetic model with R^2 of 0.944. Pseudo-second-order kinetic model assumes that surface adsorption is the rate-limiting process that involves chemisorption [54,55]. In addition, instead of adsorbate concentration, here adsorption rate is dependent

Table 1. Comparison of different kinetic models and correlation coefficients (R^2) for Pb^{2+} adsorption.

Non-linear kinetic model	Pseudo-second-order $q = (k_1*t*q_e^2)/(1+(k_1*q_e*t))$			Fractional power $q_t = K*t^v$		
	k_1 (g mg^{-1} min^{-1})	q_e (mg g^{-1})	R^2	K (mg g^{-1})	v (h^{-1})	R^2
Pristine PE + NaNO$_3$	2.850	1.239	0.944	–	–	–
Aged PE + NaNO$_3$	–	–	–	0.488	0.218	0.983

Note: k_1 is the pseudo-second-order rate constant, q_e is the equilibrium adsorption capacity, K is the fractional power constant, and v is the rate constant.

on the respective adsorption capacity. Consequently, the removal of Pb^{2+} from water is due to physiochemical interactions between the aqueous phase and PE microplastics. Nevertheless, adsorption efficiency has rapidly increased and then become stable with time as all active binding sites are occupied with Pb^{2+}.

3.7. Adsorption isotherm

The characteristics nature of Pb^{2+} adsorption behaviour on both pristine and aged with increasing the adsorbate concentration was non-linear with the introduction of ionic and organic species (Figure 6). The resultant adsorption parameters are shown in Table 2. Aged PE microplastics performed significantly reduced adsorption than pristine PE microplastics. According to the adsorption data modelling, Pb^{2+} binding onto pristine PE microplastics with the introduction of both NaNO$_3$ and HA was well described by the non-linear Freundlich isotherm model (Figure 6). However, as shown in Figure 6, Pb^{2+} adsorption onto aged PE microplastics was best fitted with non-linear Hill and Freundlich isotherm models in the presence of NaNO$_3$ and HA, correspondingly. A few studies have found that non-linear adsorption is powered by the uneven distribution of adsorption sites on the adsorbents and the pore-filling mechanism [13,56].

Hill isotherm model discusses a cooperative adsorption process on a homogeneous microplastic surface where the adsorption capacity of adsorbate at a particular binding site leads to the influence Pb^{2+} binding capacity of remaining sites [51]. Additionally, when Hill cooperative coefficient, n_H is > 1 and <1, it attributes positive and negative cooperativity in binding respectively while $n_H = 1$ indicates a non-cooperative or hyperbolic binding process [57]. Consequently, the resultant n_H of 1.364 for Pb^{2+} adsorption onto aged PE treated with NaNO$_3$ indicates a positively cooperative binding behaviour and multi-molecule adsorption where each binding site was engaged with more than one Pb^{2+} ion. Moreover, experimentally calculated positive k_H also provides an excellent indication of intermolecular interactions between the surface of microplastics and Pb^{2+} ions [58]. Therefore, it evidences the involvement of Van der Waals interactions for the Pb^{2+} binding to aged PE microplastics.

Freundlich isotherm model is generally used to describe the multilayer adsorption by forming interactions with adsorbed molecules for the heterogeneous surface energy systems [59]. The resultant adsorption curves for Pb^{2+} adsorption for pristine and aged PE microplastics displayed an upward concave shape where the measure of the intensity of adsorption, n was >1. The Freundlich model assumes that when n > 1, the adsorbates favourably bind to the heterogeneous surface while n < 1 and = 1 attribute to
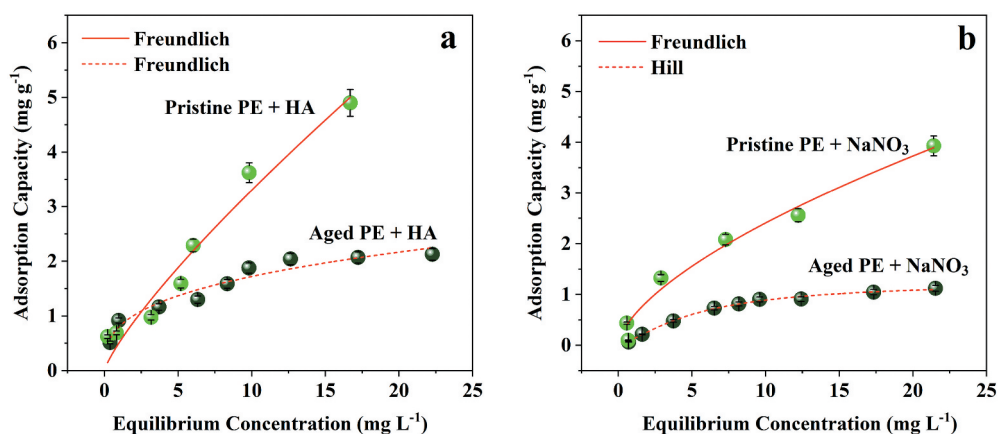
Figure 6. (a) Freundlich and Hill isotherm models for Pb^{2+} adsorption on pristine and aged PE microplastics at an initial concentration of 5 mg L^{-1} at pH range 5–6 in the presence of 0.001 M $NaNO_3$ (b) Freundlich isotherm models for Pb^{2+} adsorption on pristine and aged PE microplastics at an initial concentration of 5 mg L^{-1} at pH range 5–6 in the presence of 2.5 mg L^{-1} HA and the solid lines represent the calculated results using non-linear curve fitting.

Table 2. Adsorption isotherm parameters derived from the best fitted isotherm models.

Freundlich $Q_e = k_F C^{1/n}$	k_F ((mg g^{-1})(L g^{-1})$^{1/n}$)	n	R^2
Pristine PE + $NaNO_3$	0.562	1.583	0.979
Pristine PE + HA	0.510	1.233	0.958
Aged PE + HA	0.803	3.019	0.949
Hill	$\mathbf{Q_H}$ **(mg g^{-1})**	$\mathbf{k_H}$ **(L mg^{-1})**	$\mathbf{n_H}$	$\mathbf{R^2}$
$Q_e = (Q_H(k_H C_e)^{n_H})/(1+(k_H C_e)^{n_H})$				
Aged PE + $NaNO_3$	1.260	0.189	1.364	0.996

Note: Q_H is the Hill isotherm saturation capacity, k_H is the Hill constant, n_H is the Hill cooperativity coefficient of the binding interactions, k_F is the Freundlich constant, and n is an arbitrary constant

unfavourable and partitioning adsorbate binding [60]. In addition, when $n > 1$, the sorption is predominately facilitated through physisorption [61]. Accordingly, it can be elucidated that when increasing initial Pb^{2+} concentration, Pb^{2+} adsorption onto pristine PE microplastics in the presence of $NaNO_3$ and onto both pristine and aged PE microplastics in the presence of HA were favourably induced through multilayer physisorption. Further, several adsorption energy levels might facilitate the adsorption of Pb^{2+} onto different sites [62]. Similarly, a study has found that Pb adsorption on PP, PE, PES, PVC, and nylon microplastics was following the Freundlich model, and thereby multilayer physisorption was identified as the sorption mechanism [63]. Contrastingly, Pb^{2+} adsorption onto nylon microplastics perfectly followed Langmuir model [25]. Nevertheless, physically adsorbed toxic trace metal ions have a higher tendency to release from the microplastic surfaces.

3.8. Desorption behaviour of PE microplastics-bound Pb^{2+}

As Pb^{2+} ions were attached to PE microplastics through weak bonds, they have a higher probability to give up the surface of microplastics at a slight change of the

environmental conditions. Therefore, it is necessary to assess their desorption efficiencies by changing the specific parameters of the desorption medium. Solution pH is a critical factor that changes depending on the environment and crucially affects toxic trace metal adsorption. As illustrated in Figure 5(b), both pristine and aged microplastics-bound Pb^{2+} ions showed remarkable desorption performances when they were added to water at different pH conditions (pH 3, 5, and 7). Thus, desorption efficiency increased with increasing contact time.

Enhanced desorption efficiency of pristine microplastics-bound Pb^{2+} ions at pH 3 after 2 h (67.45%) than that of aged PE microplastics (59.12%) might be powered by more weak bonds formed during the physisorption. Also, even around the adsorption facilitating pH (i.e. pH 5), there is a considerable tendency to happen desorption. Desorption efficiency at pH 7 after 24 h (0.92%) was very low compared with others (68.13% and 6.52% at pH 7 and 5, respectively). Nevertheless, it is substantial evidence that indicates the ability of pristine PE microplastics-bound Pb^{2+} ions to desorb without depending on the pH. Microplastics can be ingested mainly by humans through food, water, and air [64]. As different systems and organs in the human body consist of different pH conditions, metal contaminants bound to ingested microplastics can be readily released inside the human body posing various health risks [25]. However, the results demonstrated that PE microplastics may act as vectors for Pb^{2+} ions through different water systems.

4. Conclusion

The present study highlights that pH, ionic species, and DOM in the sorption medium influence the ability of microplastics to adsorb and desorb co-occurring Pb^{2+}. Both PE microplastics were excellent vectors for Pb^{2+} in organic matter-rich water at pH 5–6 while ionic constituents remarkably inhibited the adsorption. The equilibrium kinetic data revealed that Pb^{2+} adsorption on pristine and aged PE microplastics was through time-dependent and rate-controlling chemisorption processes, respectively. Multilayer physisorption processes revealed by sorption isotherm data suggested that the surface complexation of Pb^{2+} onto both pristine and aged PE microplastics with the introduction of HA. The postulated possible interaction mechanism for physisorption in optimum environmental conditions was the cooperative involvement of the hydrophobic and electrostatic interactions. Physisorbed Pb^{2+} ions released the surfaces of PE microplastics at slight pH changes. All these findings imply the role of PE microplastics as vectors for the transport of Pb^{2+} through aquatic environments and risk on their co-existence. More studies focused on individual toxic trace metals that are necessary to clarify the trace metal adsorption and desorption abilities of PE microplastics with the change of different environmental conditions in aquatic environments.

Disclosure statement

Funding

ORCID

Meththika Vithanage ⓘ http://orcid.org/0000-0003-2923-4065

References

[1] A.C. Vivekanand, S. Mohapatra and V.K. Tyagi, Chemosphere. **282**, 131151 (2021). doi:10.1016/j.chemosphere.2021.131151.

[2] Y. Meng, F.J. Kelly and S.L. Wright, Environ. Pollut. **256**, 113445 (2020). doi:10.1016/j.envpol.2019.113445.

[3] Y. Peng, P. Wu, A.T. Schartup and Y. Zhang, Proc. Natl. Acad. Sci. **118** (47), e2111530118 (2021). doi:10.1073/pnas.2111530118.

[4] M. Shams, I. Alam and M.S. Mahbub, Environ. Adv. **5**, 100119 (2021). doi:10.1016/j.envadv.2021.100119.

[5] J. Duan, N. Bolan, Y. Li, S. Ding, T. Atugoda, M. Vithanage, B. Sarkar, D.C.W. Tsang and M.B. Kirkham, Water Res. **196**, 117011 (2021). doi:10.1016/j.watres.2021.117011.

[6] M. Darabi, H. Majeed, A. Diehl, J. Norton and Y. Zhang, Curr. Pollut. Rep. **7**, 40–53 (2021).

[7] M. Sewwandi, O. Hettithanthri, S.M. Egodage, A.A.D. Amarathunga and M. Vithanage, Sci. Total Environ. **828**, 154374 (2022). doi:10.1016/j.scitotenv.2022.154374.

[8] M. Ahechti, M. Benomar, M. El Alami and C. Mendiguchía, J. Environ. Anal. Chem. **102**, 1118–1125 (2020).

[9] T. Atugoda, H. Wijesekara, D.R.I.B. Werellagama, K.B.S.N. Jinadasa, N.S. Bolan and M. Vithanage, Environ. Technol. Innov. **19**, 100971 (2020). doi:10.1016/j.eti.2020.100971.

[10] Y. Cao, M. Zhao, X. Ma, Y. Song, S. Zuo, H. Li and W. Deng, Sci. Total Environ. **788**, 147620 (2021). doi:10.1016/j.scitotenv.2021.147620.

[11] T. Atugoda, M. Vithanage, H. Wijesekara, N. Bolan, A.K. Sarmah, M.S. Bank, S. You and Y.S. Ok, Environ. Int. **149**, 106367 (2021). doi:10.1016/j.envint.2020.106367.

[12] M. Carbery, W. O'Connor and T. Palanisami, Environ. Int. **115**, 400–409 (2018). doi:10.1016/j.envint.2018.03.007.

[13] Y. Dong, M. Gao, Z. Song and W. Qiu, Chemosphere. **239**, 124792 (2020). doi:10.1016/j.chemosphere.2019.124792.

[14] N. Khalid, M. Aqeel, A. Noman, S.M. Khan and N. Akhter, Environ. Pollut. **290**, 118104 (2021). doi:10.1016/j.envpol.2021.118104.

[15] Q. Fu, X. Tan, S. Ye, L. Ma, Y. Gu, P. Zhang, Q. Chen, Y. Yang and Y. Tang, Chemosphere. **270**, 128624 (2021). doi:10.1016/j.chemosphere.2020.128624.

[16] Q. Wang, Y. Zhang, X. Wangjin, Y. Wang, G. Meng and Y. Chen, J. Environ. Sci. **87**, 272–280 (2020). doi:10.1016/j.jes.2019.07.006.

[17] H. Luo, Y. Zhao, Y. Li, Y. Xiang, D. He and X. Pan, Sci. Total Environ. **714**, 136862 (2020). doi:10.1016/j.scitotenv.2020.136862.

[18] S. Abbasi and A. Turner, J. Hazard. Mater. **403**, 123799 (2021). doi:10.1016/j.jhazmat.2020.123799.

[19] K.D. Cox, G.A. Covernton, H.L. Davies, J.F. Dower, F. Juanes and S.E. Dudas, Environ. Sci. Technol. **53** (12), 7068–7074 (2019). doi:10.1021/acs.est.9b01517.

[20] S. Abarghouei, A. Hedayati, M. Raeisi, B.S. Hadavand, H. Rezaei and A. Abed-Elmdoust, Chemosphere. **276**, 129977 (2021). doi:10.1016/j.chemosphere.2021.129977.

[21] S. D'Angelo and R. Meccariello, Int J Environ. Res. Public Health. **18** (5), 2392 (2021). doi:10.3390/ijerph18052392.

[22] R. Zhang, V.L. Wilson, A. Hou and G. Meng, Int. J. Health Animal Sci. Food Saf. **2** (1), 18–31 (2015).

[23] B. Hartono and R.S.M. Pratiwi, Open Access Maced. J. Med. Sci. **9** (E), 1413–1417 (2021). doi:10.3889/oamjms.2021.7530.

[24] L. Lin, S. Tang, X. Wang, X. Sun and A. Yu, Chemosphere. **265**, 129079 (2021). doi:10.1016/j.chemosphere.2020.129079.

[25] S. Tang, L. Lin, X. Wang, A. Feng and A. Yu, J. Hazard. Mater. **386**, 121960 (2020). doi:10.1016/j.jhazmat.2019.121960.

[26] M. Shen, B. Song, G. Zeng, Y. Zhang, F. Teng and C. Zhou, J. Chem. Eng. **405**, 126989 (2021). doi:10.1016/j.cej.2020.126989.

[27] X. Huang, D.Y. Zemlyanov, S. Diaz-Amaya, M. Salehi, L. Stanciu and A.J. Whelton, J. Hazard. Mater. **385**, 121585 (2020). doi:10.1016/j.jhazmat.2019.121585.

[28] D. Brennecke, B. Duarte, F. Paiva, I. Caçador and J. Canning-Clode, Estuar. Coast. Shelf. Sci. **178**, 189–195 (2016). doi:10.1016/j.ecss.2015.12.003.

[29] M. Llorca, G. Schirinzi, M. Martínez, D. Barceló and M. Farré, Environ. Pollut. **235**, 680–691 (2018). doi:10.1016/j.envpol.2017.12.075.

[30] X. Guo, X. Wang, X. Zhou, X. Kong, S. Tao and B. Xing, Environ. Sci. Technol. **46** (13), 7252–7259 (2012). doi:10.1021/es301386z.

[31] H. Zhang, S. Pap, M.A. Taggart, K.G. Boyd, N.A. James and S.W. Gibb, Environ. Pollut. **258**, 113698 (2020). doi:10.1016/j.envpol.2019.113698.

[32] R.P. Di Amelia, S. Gentile, W.F. Nirode and L. Huang, World J. Chem. Educ. **4** (2), 25–31 (2016).

[33] X. Guo and J. Wang, Environ. Pollut. **250**, 737–745 (2019). doi:10.1016/j.envpol.2019.04.091.

[34] J. Brandon, M. Goldstein and M.D. Ohman, Mar. Pollut. Bull. **110** (1), 299–308 (2016). doi:10.1016/j.marpolbul.2016.06.048.

[35] N. Girard-Perier, S. Dorey, F. Gaston, F. Girard, S.R.A. Marque and N. Dupuy, Polym. Degrad. Stab. **195**, 109790 (2022). doi:10.1016/j.polymdegradstab.2021.109790.

[36] S.R. Ryu, I. Noda and Y.M. Jung, Appl. Spectrosc. **64** (9), 1017–1021 (2010). doi:10.1366/000370210792434396.

[37] A. de Vos, L. Aluwihare, S. Youngs, M.H. DiBenedetto, C.P. Ward, A.P.M. Michel, B.C. Colson, M.G. Mazzotta, A.N. Walsh, R.K. Nelson, C.M. Reddy and B.D. James, ACS Environ. Au. **2** (2), 128–135 (2021). doi:10.1021/acsenvironau.1c00031.

[38] R. Bardestani, C. Roy and S. Kaliaguine, J. Environ. Manage. **240**, 404–420 (2019). doi:10.1016/j.jenvman.2019.03.110.

[39] X.S. Wang, H.J. Lu, L. Zhu, F. Liu and J.J. Ren, Adsorpt. Sci. Technol. **28** (5), 407–417 (2010). doi:10.1260/0263-6174.28.5.407.

[40] L.A. Holmes, A. Turner and R.C. Thompson, Environ. Pollut. **160** (1), 42–48 (2012). doi:10.1016/j.envpol.2011.08.052.

[41] L.A. Holmes, A. Turner and R.C. Thompson, Mar. Chem. **167**, 25–32 (2014). doi:10.1016/j.marchem.2014.06.001.

[42] X. Guo, G. Hu, X. Fan and H. Jia, Ecotoxicol. Environ. Saf. **190**, 110118 (2020). doi:10.1016/j.ecoenv.2019.110118.

[43] B. Xu, F. Liu, P.C. Brookes and J. Xu, Mar. Pollut. Bull. **131**, 191–196 (2018). doi:10.1016/j.marpolbul.2018.04.027.

[44] E. Eren and B. Afsin, Dyes. Pigm. **73** (2), 162–167 (2007). doi:10.1016/j.dyepig.2005.11.004.

[45] M.F. Torres, J.M. González, M.R. Rojas, A.J. Müller, A.E. Sáez, D. Löf and K. Schillén, J. Colloid Interface Sci. **307** (1), 221–228 (2007). doi:10.1016/j.jcis.2006.11.002.

[46] K. Vermöhlen, H. Lewandowski, H.D. Narres and M.J. Schwuger, Colloids Surf. A Physicochem. Eng. Asp. **163** (1), 45–53 (2000). doi:10.1016/S0927-7757(99)00429-X.

[47] P. Hemalatha and M.V.M. Desal, Speciation of humic acid and some transition metal ions in presence of each other under alkaline pH conditions, (Head, Library and Information Services Division, Bhabha Atomic Research Centre, Mumbai, India, 1998). BARC External. https://www.osti.gov/etdeweb/servlets/purl/335912.

[48] W. Chen, H. Sandoval, J.Z. Kubiak, X.C. Li, R.M. Ghobrial and M. Kloc, Cell. Immunol. **324**, 1–7 (2018). doi:10.1016/j.cellimm.2017.11.003.

[49] J. Xu, W. Tan, J. Xiong, M. Wang, L. Fang and L.K. Koopal, J. Colloid Interface Sci. **473**, 141–151 (2016). doi:10.1016/j.jcis.2016.03.066.

[50] X.L. Tan, P.P. Chang, Q.H. Fan, X. Zhou, S.M. Yu, W.S. Wu and X.K. Wang, Colloids Surf. A Physicochem. Eng. Asp. **328** (1), 8–14 (2008). doi:10.1016/j.colsurfa.2008.06.022.

[51] A. Ashiq, B. Sarkar, N. Adassooriya, J. Walpita, A.U. Rajapaksha, Y.S. Ok and M. Vithanage, Chemosphere **236**, 124384 (2019). doi:10.1016/j.chemosphere.2019.124384.

[52] S. Álvarez-Torrellas, R.S. Ribeiro, H.T. Gomes, G. Ovejero and J. García, J. Chem. Eng. **296**, 277–288 (2016). doi:10.1016/j.cej.2016.03.112.

[53] A.O. Dada, F. Adekola and E. Odebunmi, Appl. Water Sci. **7** (3), 1409–1427 (2017). doi:10.1007/s13201-015-0360-5.

[54] A. Murcia-Salvador, J.A. Pellicer, M.I. Fortea, V.M. Gómez-López, M.I. Rodríguez-López, E. Núñez-Delicado and J.A. Gabaldón, Polymers. **11** (6), 1003 (2019). doi:10.3390/polym11061003.

[55] D. Robati, J. Nanostruct. Chem. **3** (1), 1–6 (2013). doi:10.1186/2193-8865-3-55.

[56] S. Ahn, D. Werner, H.K. Karapanagioti, D.R. McGlothlin and R.N. Zare, R. G. J. E. S. Luthy Technol. Environ. Sci. Technol. **39** (17), 6516–6526 (2005). doi:10.1021/es050113o.

[57] N. Sivarajasekar and R. Baskar, Arab. J. Chem. **12** (7), 1322–1337 (2019). doi:10.1016/j.arabjc.2014.10.040.

[58] G. Lin, T. Hu, S. Wang, T. Xie, L. Zhang, S. Cheng, L. Fu and C. Xiong, Chemosphere. **225**, 65–72 (2019). doi:10.1016/j.chemosphere.2019.03.006.

[59] A. Bozorgian, Chem. Rev. Lett **3** (2), 79–85 (2020).

[60] R.-L. Tseng and F.-C. Wu, J. Hazard. Mater. **155** (1), 277–287 (2008). doi:10.1016/j.jhazmat.2007.11.061.

[61] M.B. Desta, J. Thermodyn. **2013**, 375830 (2013). doi:10.1155/2013/375830.

[62] N.F. Zon, A. Iskendar, S. Azman, S. Sarijan and R. Ismail, MATEC Web of Conferences, EDP Sciences, (2018), Vol. 250, p. 06001.

[63] A.I.S. Purwiyanto, Y. Suteja, T.P.S. Ningrum, W.A.E. Putri, F.A. Rozirwan, M.R.C. Fauziyah and A.F. Koropitan, Mar. Pollut. Bull. **158**, 111380 (2020). doi:10.1016/j.marpolbul.2020.111380.

[64] L. Bradney, H. Wijesekara, K.N. Palansooriya, N. Obadamudalige, N.S. Bolan, Y.S. Ok, J. Rinklebe, K.H. Kim and M.B. Kirkham, Environ. Int. **131**, 104937 (2019). doi:10.1016/j.envint.2019.104937.